Critical exponents and phase diagram of polymer blend solutions: polystyrene/poly(methyl methacrylate)/d_6-benzene system

Naoshi Miyashita, Mamoru Okada and Takuhei Nose*

Department of Polymer Chemistry, Tokyo Institute of Technology, Ookayama, Meguro-ku, Tokyo 152, Japan

(Received 29 March 1993)

Critical behaviour of blend solutions of polystyrene ($M_w = 3.55 \times 10^5$)/poly(methyl methacrylate) ($M_w = 3.27 \times 10^5$) in d_6-benzene was investigated by static light scattering. The phase diagram (spinodal, binodal and cloud points) was determined at a fixed total polymer concentration. The system had the lower critical solution temperature. The inverse isothermal osmotic compressibility $(\partial\pi/\partial c_1)_T$ and correlation length ξ of concentration fluctuations were determined as functions of the reduced temperature $\varepsilon = |T_s/T - 1|$ near the stability limit, where T is the absolute temperature and T_s is the spinodal temperature. Both $(\partial\pi/\partial c_1)_T$ and ξ were described by single exponents over the investigated temperature range. The critical exponents γ and ν for $(\partial\pi/\partial c_1)_T$ and ξ were 1.23 and 0.63, respectively. They were very close to the three-dimensional Ising exponents and obviously different from the mean-field or Fisher's renormalized Ising exponents, as theoretically predicted by Broseta *et al.*

(Keywords: polymer blend solution; critical behaviour; three-dimensional Ising model)

INTRODUCTION

A fluid mixture containing polymers is an interesting system for studying critical phenomena, because it has a wider critical region than mixtures of small molecules, and because a polymeric mixture may show somewhat different behaviour from ordinary fluid mixtures, although the characteristic feature of critical phenomena lies in their universality independent of the system. Generally, critical phenomena can be classified into several universality classes, and both theoretical and experimental studies[1–12] have been made to determine the class to which a polymeric system belongs. In a theoretical letter of de Gennes[1], the applicability of the classical mean-field theory near the critical point was discussed for the segregation of mixtures containing long, flexible polymer chains. The temperature interval ΔT^* in which the non-classical critical behaviour was observed was estimated, and the following results for three cases of polymer systems were obtained:

(a) *Binary polymer solution* (polymer/poor solvent). The non-classical region ranges over $\Delta T^* \simeq \Theta - T_c$ with Θ being the theta temperature and T_c the critical temperature. In the entire temperature range from Θ to T_c, where polymers tend to segregate, the mean-field theory cannot describe the critical behaviour.

(b) *Polymer blend* (polymer A/polymer B). For a symmetric system consisting of two polymers with the same degree of polymerization N, it holds that $\Delta T^* \simeq (T_0 - T_c)N^{-1}$, where T_0 is the compensation temperature at which the interaction vanishes. If N is large enough, the mean-field theory is valid in most of the temperature range from T_0 to T_c.

(c) *Polymer blend solution* (polymer A/polymer B/good solvent). Suppose a semidilute blend solution where the total polymer concentration c is larger than the overlap concentration c^*. If segregation between polymers A and B is strong enough, the blend solution separates into two phases having approximately the same polymer concentration but different polymer composition. The critical behaviour was presumed to be non-classical for this case.

Thus far several experimental studies for binary polymer solutions[2,3] and polymer blends[5–10] have been reported, and the results were consistent with the above predictions. Theoretical evaluation of ΔT^* for an asymmetric polymer blend was made by Bates *et al.*[7]. A recent study for polyisoprene/poly(ethylene–propylene) mixtures by Stepanek *et al.*[8] has shown that the crossover from classical mean-field to non-classical behaviour occurs with temperature approaching the spinodal temperature T_s, and that ΔT^* was well described by the theory[7]. To our knowledge, no experimental study has been made of the critical phenomena for polymer blend solutions (case (c)), which we study in this work.

A quantitative evaluation of ΔT^* for polymer blend solutions has been made by Broseta *et al.*[11], who derived an expression based on the Ginzburg criterion and the blob model of a quasi-binary mixture. They concluded that, as long as the value of c_c/c^* is not too much larger than unity, which is the case for most systems, the non-classical region is expected to be observed over a

* To whom correspondence should be addressed

0032-3861/94/05/1038–06

quite wide temperature range. Here c_c is the total polymer concentration at the critical point and the overlap concentration c^* is defined as:

$$c^*(\text{vol/vol}) \equiv M/(4\pi R_F^3 \rho N_A/3)$$

where ρ is density, R_F is the radius of gyration of the polymer at infinite dilution, and N_A is the Avogadro number. A similar conclusion has been reached by Benmouna *et al.*[12], who used the blob concept and the theory of Bates *et al.*[7].

Critical behaviour is usually characterized by the critical exponents. The critical exponents for the osmotic susceptibility S and the correlation length ξ are defined as:

$$S \propto \left(\frac{|\chi-\chi_s|}{\chi_s}\right)^{-\gamma} \propto \left|\frac{T_s}{T}-1\right|^{-\gamma} \quad (1)$$

$$\xi \propto \left(\frac{|\chi-\chi_s|}{\chi_s}\right)^{-\nu} \propto \left|\frac{T_s}{T}-1\right|^{-\nu} \quad (2)$$

Here, χ represents the Flory–Huggins interaction parameter, T is the absolute temperature, and χ_s is χ at the spinodal temperature T_s. The classical mean-field theory predicts that these critical exponents should have the values $\gamma=1$ and $\nu=1/2$, whereas they should take the three-dimensional Ising (3D Ising) values i.e. $\gamma=1.24$ and $\nu=0.63$[13], in the non-classical region of fluid systems. The critical exponents of the non-classical region have in fact been observed in binary polymer solutions (case (a))[2,3] and polymer blends (case (b))[5–10].

In ternary mixtures such as blend solutions, the situation is more complex. In a mixture of polymer A/polymer B/solvent, there exists a small fluctuation of total polymer concentration c besides that of polymer composition (the ratio of polymer A/polymer B). The 3D Ising exponents are observed only if T approaches T_s (or T_c) with a fixed chemical potential of both polymers, that is, if the observed fluctuation is only in the polymer composition. However, under practical experimental conditions with a fixed total polymer concentration, fluctuations of the total polymer concentration become appreciable in the vicinity of the critical point. The divergence of concentration fluctuations is expected to result in a shift of T_s and the appearance of Fisher's renormalized Ising exponents[14]. The exponents γ and ν become γ^* and ν^* given as $\gamma^*=\gamma/(1-\alpha)$ and $\nu^*=\nu/(1-\alpha)$. Here α is the critical exponent of the heat capacity, taking the value of 0.11[13]. The renormalized exponents have been observed in ternary mixtures of small molecules[15]. According to the theory of Broseta *et al.*[11] for blend solution systems, however, the temperature interval $\Delta T^{**}/T_s$ in which the renormalized Ising exponents may be observed is negligibly small, and the critical exponents are expected not be be of the renormalized Ising type, but of the 3D Ising type.

Figure 1 summarizes the theoretical prediction of

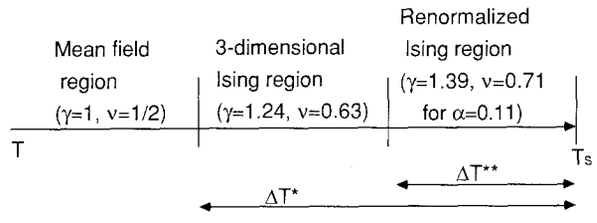

Figure 1 Universality classes in the temperature region near the spinodal temperature T_s of polymer A/polymer B/good solvent systems

Table 1 Characteristics, cloud temperature T_{cl} and spinodal temperature T_s of PS/PMMA/d_6-Bz mixtures

Sample code	c (vol%)	PS/PMMA[a]	T_{cl} (°C)	T_s (°C)
PS22	8.15	22.0/78.0		
PS25	8.16	24.9/75.1	40.6–43.6	62.7
PS32	8.17	32.0/68.0		
PS36	8.19	35.8/64.2		
PS42	8.19	41.5/58.5	31.4–31.6	32.7
PS53	8.29	52.6/47.4	24.1–25.1	26.0
PS63	8.37	63.4/36.6	26.3–28.4	32.8

[a] Volume ratio

universality classes in a temperature region near the spinodal temperature T_s in a polymer A/polymer B/good solvent system. The main purpose of this paper is to elucidate the universality class of a polymer blend solution. We have selected polystyrene/poly(methyl methacrylate)/d_6-benzene as the sample and found that the system has a lower critical solution temperature (*LCST*). Values of γ and ν have been determined by means of static light scattering, and compared with the theory of Broseta *et al.*[11].

EXPERIMENTAL

Materials

Polystyrene (PS) was a product of Tosoh Co. and its weight-average molecular weight M_w and polydispersity index M_w/M_n were 3.55×10^5 and 1.02, respectively. Poly(methyl methacrylate) (PMMA) with $M_w=3.27\times10^5$ and $M_w/M_n\leqslant1.10$ was a product of Pressure Chemical Co. Deuterated benzene (d_6-Bz) with 99.7% deuteration was purchased from Merck Sharp & Dohme Co., and purified by distillation under reduced pressure.

Sample preparation

Deuterated benzene solutions with a fixed total polymer concentration of 8.2 vol% were prepared as follows. Known amounts of PS and PMMA were first dissolved in hydrogenated benzene to make a dilute solution that was filtered with a Millipore filter of 0.22 μm pore diameter into a glass tube of 4.2 mm inner diameter. After removal of hydrogenated benzene by evaporation under vacuum, d_6-Bz was added through a filter into the sample tube to make a solution of the desired concentration. The sample tube was flame sealed after air in the tube was replaced with nitrogen gas. The samples thus prepared are listed in *Table 1*.

Light scattering

Details of the light scattering apparatus are described elsewhere[16]. An argon-ion laser operated at 488.0 nm was used as the light source. A sample tube was immersed in an index-matched oil bath whose temperature was controlled to 0.05°C. Turbidity τ was calculated from the Rayleigh ratio[17] to be 1.6×10^{-1} cm^{-1} in the maximum case; thus attenuation τd, where optical path $d=0.42$ cm, of the scattered light was less than 7.0×10^{-2}. In most cases τd was less than 2×10^{-2} and had a negligible effect on the determination of the critical exponents. Theoretical calculation has shown that the multiple scattering effect is of the same order as or less than attenuation[18]. Thus no correction of scattered intensity was made for attenuation and multiple scattering.

Most of the scattered light intensity comes from fluctuation of PS/PMMA composition near the critical point: in the temperature range where PS/PMMA/d_6-Bz solution showed critical behaviour, the scattering intensity of a binary PS/d_6-Bz solution of the same polymer concentration was confirmed to be 1/100 to 1/1000 times that of PS/PMMA/d_6-Bz. The wavenumber q dependence of the integrated scattered intensity $I(q)$ was well described by the Ornstein–Zernike equation:

$$I(0)/I(q) = 1 + q^2\xi^2 \tag{3}$$

as indicated by the good linear relation between $I^{-1}(q)$ and q^2 shown in *Figure 2*, where the results of the sample PS42 are presented as examples. Correlation length ξ and $I^{-1}(0)$ were determined from $I(q)$ by least-squares fitting to the Ornstein–Zernike equation (3).

Since d_6-Bz, whose refractive index is 1.51[19], is regarded as an isorefractive solvent of PMMA, the scattered intensity $I(q)$ is proportional to the structure function $S_{11}(q) = \langle \delta c_1(q) \delta c_1(-q) \rangle$, where $\delta c_1(q)$ is the Fourier transform of the concentration fluctuation of PS (component 1). $S_{11}(0)$ is related to the inverse osmotic compressibility $(\partial\pi/\partial c_1)_T$ and thus:

$$\frac{c_1}{I(0)} \propto \frac{c_1}{S_{11}(0)} = \frac{v}{k_B T}\left(\frac{\partial \pi}{\partial c_1}\right) \tag{4}$$

where k_B is the Boltzmann constant and v is the volume of the monomer. It must be noted that isorefractivity of d_6-Bz to PMMA is not a condition to be strictly satisfied as long as we do not discuss absolute values of osmotic compressibility, because it has been suggested that all structure functions $S_{ij} = \langle c_i \delta c_j \rangle$ diverge in the same way[12]. On the basis of equation (4), the inverse osmotic compressibility $(\partial\pi/\partial c_1)_T$ or inverse susceptibility S^{-1} was evaluated in an arbitrary scale:

$$(\partial\pi/\partial c_1)_T \sim T/I(0) \tag{5}$$

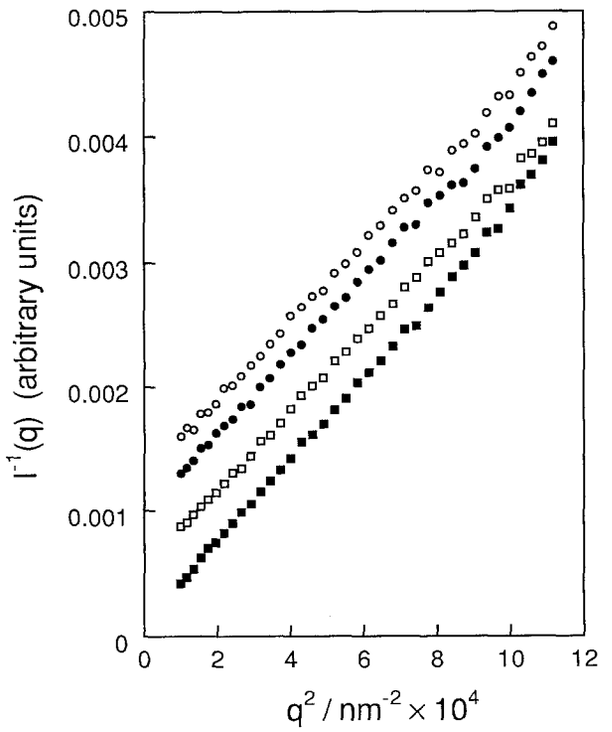

Figure 2 Ornstein–Zernike plots of $I^{-1}(q)$ vs. q^2 for PS42: (○) 20.2°C; (●) 22.1°C; (□) 26.2°C; (■) 30.9°C

Binodal

Coexisting compositions were determined from volume ratios of two coexisting phases. We neglected the difference in solvent goodness for both component polymers in the calculation and assumed that coexisting phases had the same total polymer concentration.

RESULTS AND DISCUSSION

Figures 3 and *4* show the temperature dependences of $(\partial\pi/\partial c_1)_T$ and ξ, respectively. As temperature T approached the stability limit, $(\partial\pi/\partial c_1)_T$ decreased to zero and ξ diverged. It was observed that $(\partial\pi/\partial c_1)_T$ of PS53 and PS63 increased again at high temperature. Corresponding to this upturn in $(\partial\pi/\partial c_1)_T$, a downturn in ξ was observed at high temperature. Similar phenomena were observed in polymer blends[5,6,10] and attributed to phase separation. These inflection points were taken as cloud points T_{cl}. The spinodal temperature T_s, together with the critical exponent γ for susceptibility, was determined by fitting the data of $(\partial\pi/\partial c_1)_T$ to the following equation:

$$\left(\frac{\partial \pi}{\partial c_1}\right)_T = \left(\frac{\partial \pi}{\partial c_1}\right)_{T_0} \varepsilon^{\gamma} \tag{6}$$

where ε is defined by:

$$\varepsilon = |T_s/T - 1| \tag{7}$$

The cloud temperatures T_{cl} and the spinodal temperatures T_s are listed in *Table 1* and shown in *Figure 5*. In *Figure 5*, coexisting compositions at a fixed total polymer concentration 8.2 vol% are also shown. Abscissa Φ_{PS} is composition of PS, i.e. volume fraction of PS in the total volume of polymers ($\Phi_{PS} + \Phi_{PMMA} = 1$). The solution was miscible at lower temperatures and the lower critical point was estimated to be $\Phi_c = 0.48 \pm 0.02$ and $T_c \simeq 27$°C from both the intersection of the line connecting the midpoints of tie lines with the binodal curve and the point where the binodal curve contacts with the spinodal curve. The critical concentration appeared to be consistent with the results of other works[20–22], as shown in *Figure 6*, where the critical total polymer concentration c_c, at temperatures relatively close to the present T_c, of hydrogenated benzene solutions of blends of PS and PMMA having approximately the same molecular weights are plotted against the average molecular weight of polymers in double-logarithmic scale. It is observed that the phase diagram has asymmetric shape, which is considered to reflect asymmetry in the solvent goodness of d_6-Bz for both polymers, because hydrogenated benzene is known to have a slightly stronger affinity for PS than for PMMA. The *LCST*-type phase diagram suggests a positive temperature dependence of the interaction parameter $\chi_{PS/PMMA}$ between PS and PMMA in benzene solution, while a negative temperature dependence of $\chi_{PS/PMMA}$ in the bulk system has been reported by Higashida *et al.*[23,24]. They estimated $\chi_{PS/PMMA}$ from interfacial thickness measured by ellipsometry and referred to the unpublished work by Ougisawa, who obtained a *UCST*-type phase diagram for a blend of low-molecular-weight PS and PMMA. Using the evaluated T_s, the critical exponent ν for the correlation length ξ was determined by fitting ξ to the equation:

$$\xi = \xi_0 \varepsilon^{-\nu} \tag{8}$$

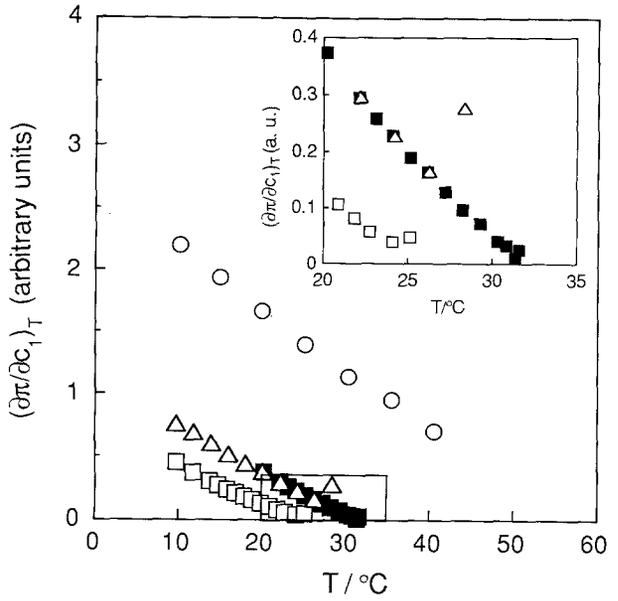

Figure 3 Temperature dependence of the inverse isothermal osmotic compressibility $(\partial\pi/\partial c_1)_T$ for samples: (○) PS25; (■) PS42; (□) PS53; (△) PS63. The inset shows an enlargement of the region near $(\partial\pi/\partial c_1)_T = 0$

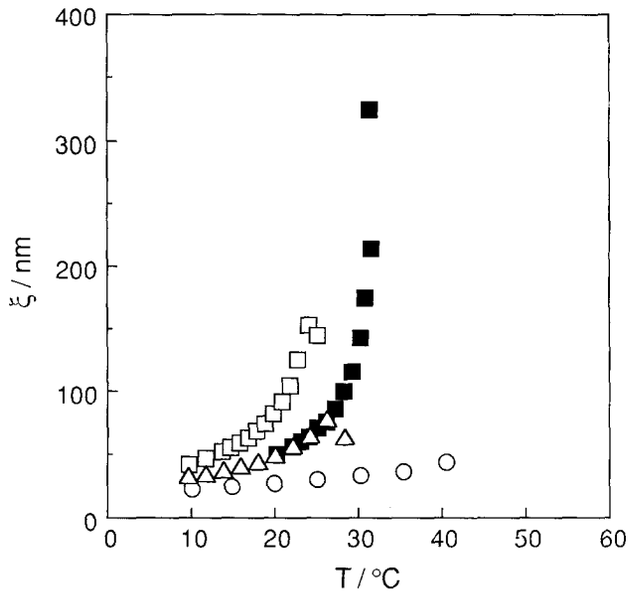

Figure 4 Temperature dependence of correlation length ξ. Symbols are the same as in *Figure 3*

The critical exponents γ and ν and the prefactor are listed in *Table 2*.

Figures 7 and *8* show double-logarithmic plots of $(\partial\pi/\partial c_1)_T$ and ξ respectively against ε. All plots show good linearity, which indicates that $(\partial\pi/\partial c_1)_T$ and ξ are well described by power laws. Although the exponent γ seemed to decrease slightly and the exponent ν seemed to increase slightly as the composition departed from the critical one, γ and ν for four different compositions were approximately the same, as seen in *Table 2*. We obtained $\gamma = 1.20$ and $\nu = 0.65$ as mean values of all four data, and $\gamma = 1.23$ and $\nu = 0.63$ as mean values of two data for compositions (S42, S53) close to the critical point. These are very close to those of the 3D Ising model ($\gamma = 1.24$ and $\nu = 0.63$), and obviously different from those of the mean-field model ($\gamma = 1$ and $\nu = 1/2$) or the renormalized Ising model ($\gamma^* = 1.39$ and $\nu^* = 0.71$ for $\alpha = 0.11$). We observed only a 3D Ising region in the investigated temperature range and Fisher's

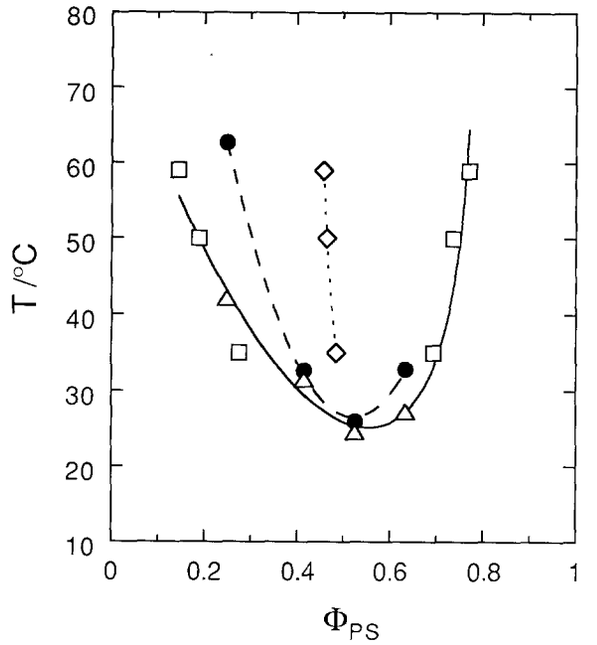

Figure 5 Phase diagram of PS/PMMA/d_6-Bz system at a fixed total polymer concentration 8.2 vol%. Φ_{PS} on the abscissa is PS composition in the total volume of polymers. Symbols: (□) binodal points; (△) cloud points; (●) spinodal points; (◇) midpoints of binodal points (diameter)

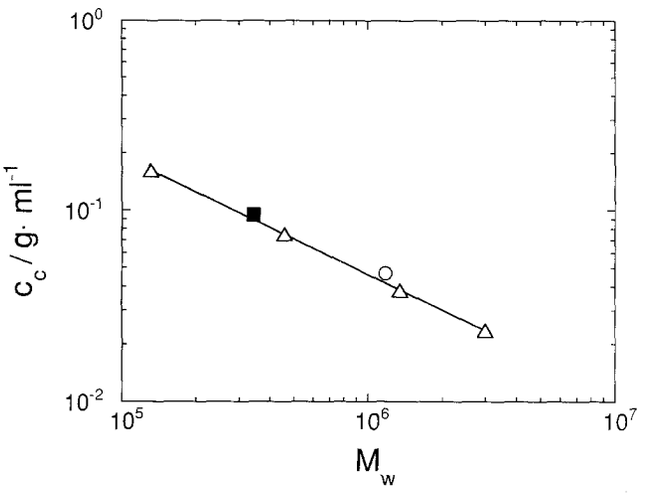

Figure 6 Plots of critical total polymer concentration c_c against molecular weight M_w around room temperature for hydrogenated or deuterated benzene solution of symmetrical PS/PMMA blend. M_w on the abscissa is the average of molecular weights of PS and PMMA. Symbols: (△) hydrogenated benzene solution (Kaddour *et al.*[20,21]); (○) hydrogenated benzene solution (Okada *et al.*[22]); (■) deuterated benzene solution (this work); (——) prediction by the renormalization group theory ($c_c \sim M_w^{-0.63}$)

Table 2 Critical exponents, prefactor and investigated range of ξ

Sample code	γ	ν	$(\partial\pi/\partial c_1)_{T_0}$[a]	ξ_0 (nm)	$\xi(c)/\xi \times 10^2$
PS25	1.18_0	0.65_4	16.0	7.65	4.39–8.43
PS42	1.25_6	0.62_8	19.6	6.91	0.59–3.87
PS53	1.20_3	0.64_0	13.6	6.88	1.26–4.57
PS63	1.16_4	0.66_0	14.1	6.28	2.45–5.78

[a] In arbitrary units

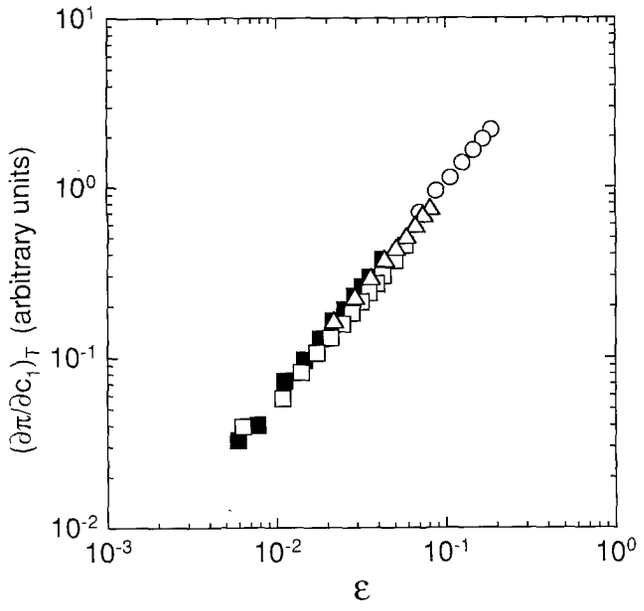

Figure 7 Double-logarithmic plots of $(\partial\pi/\partial c_1)_T$ vs. ε. Symbols are the same as in *Figure 3*

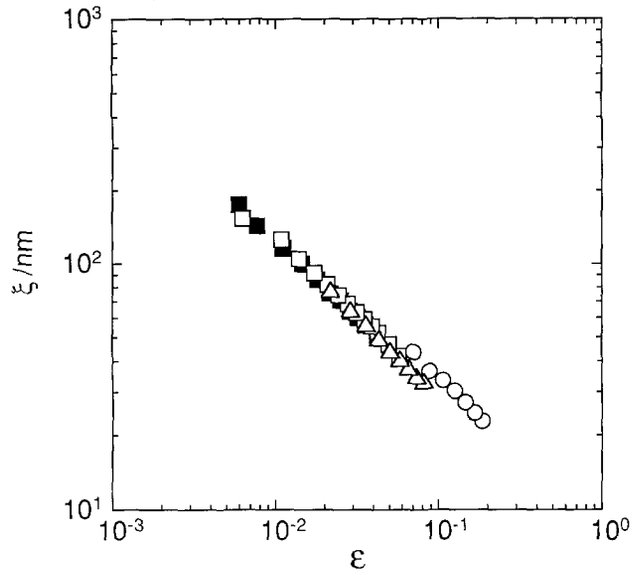

Figure 8 Double-logarithmic plots of ξ vs. ε. Symbols are the same as in *Figure 3*

renormalization effect was not detectable in the critical scattering, though slight asymmetry in the solvent affinity exists in the system. This is consistent with the theoretical prediction by Broseta *et al.*[11]. That is, the critical behaviour of a polymer/polymer/good solvent system can be described by the 3D Ising model under practical experimental conditions. Based on the Ginzburg criterion, Broseta *et al.*[11] derived expressions of ΔT^* and ΔT^{**} for a symmetric blend solution:

$$\frac{\Delta T^*}{T_s}=\frac{|\chi^*-\chi_s|}{\chi_s}=\frac{16\pi^2}{3K_R^3}\left(\frac{c_c}{c^*}\right)^{-1/(3\sigma-1)} \tag{9}$$

$$\frac{\Delta T^{**}}{T_s}=\frac{|\chi^{**}-\chi_s|}{\chi_s}=\left(\frac{\xi(c)}{R_g(c)}\right)^{3/\alpha} \tag{10}$$

where σ ($\simeq 0.588$) is the swelling exponent defined by $R_F \sim M^\sigma$ with radius of gyration R_F of an isolated polymer chain in a good solvent, K_R is a universal constant independent of the system, and $R_g(c)$ is radius of gyration in a semidilute solution, which is related to c by:

$$\frac{R_g^2(c)}{R_F^2}=K_R\left(\frac{c_5 c}{c^*}\right)^{-(2\sigma-1)/(3\sigma-1)} \tag{11}$$

Equations (9) and (10) can be transformed to expressions for correlation lengths ξ_T and $\xi_{T^{**}}$ of composition fluctuation, if the mean-field exponent is assumed for divergence of ξ_T:

$$\xi_T=\frac{R_g(c)}{\sqrt{3}}\left(\frac{|\chi-\chi_s|}{\chi_s}\right)^{-1/2} \tag{12}$$

That is, from equations (9)–(12) and the equation:

$$\frac{\xi(c)}{R_F}=K_\xi\left(\frac{c_c}{c^*}\right)^{-\sigma/(3\sigma-1)} \tag{13}$$

for the correlation length $\xi(c)$ of concentration fluctuation in a good-solvent semidilute solution far from the critical point, we obtain:

$$\frac{\xi(c)}{\xi_T^*}=\frac{4\pi K_\xi}{K_R^2}\left(\frac{c_c}{c^*}\right)^{-1/(3\sigma-1)} \tag{14}$$

$$\frac{\xi(c)}{\xi_T^{**}}=\sqrt{3}\left(\frac{K_\xi}{K_R^{1/2}}\right)^{(2\alpha+3)/2\alpha}\left(\frac{c_c}{c^*}\right)^{-(2\alpha+3)/4\alpha(3\sigma-1)} \tag{15}$$

where K_ξ is another universal constant. K_R and K_ξ have been calculated by the direct renormalization theory[11,25,26] to be 1.4 and 0.5, respectively. With numerical values for σ, K_R, K_ξ and $\alpha=0.11$, equations (14) and (15) yield:

$$\frac{\xi(c)}{\xi_T^*}=3.21\left(\frac{c_c}{c^*}\right)^{-1.31} \tag{16}$$

$$\frac{\xi(c)}{\xi_T^{**}}=5.80\times 10^{-6}\left(\frac{c_c}{c^*}\right)^{-9.58} \tag{17}$$

respectively. The value of c_c/c^* was estimated to be 12.9 in the present case by using the values $M_w=3.55\times 10^5$ and $R_F\simeq 27.5$ nm (ref. 27). Then, we obtain $\xi(c)/\xi_{T^*}=0.113$ and $\xi(c)/\xi_{T^{**}}=1.34\times 10^{-15}$. Since the experimental value of ξ is considered to be almost identical with ξ_T, we can compare the value range of $\xi(c)/\xi$, which is listed in *Table 2*, with $\xi(c)\xi_{T^*}$ and $\xi(c)/\xi_{T^{**}}$. Higher bounds of $\xi(c)/\xi$ are sufficiently smaller than $\xi(c)/\xi_{T^*}$ and lower bounds are extremely larger than $\xi(c)/\xi_{T^{**}}$. Therefore, we have to carry out measurement at much lower temperatures or in a more concentrated solution in order to observe the mean-field region.

REFERENCES

1 de Gennes, P. G. *J. Phys. Lett.* 1977, **38**, L411
2 Hamano, K., Kuwahara, T. and Kaneko, M. *Phys. Rev. (A)* 1980, **21**, 1312
3 Hamano, K., Nomura, T., Kawazura, T. and Kuwahara, N. *Phys. Rev. (A)* 1982, **26**, 1153
4 Joanny, J. F. *J. Phys. (A) Math. Gen.* 1978, **11**, L117
5 Schwann, D., Mortensen, K. and Yee-Maderia, H. *Phys. Rev. Lett.* 1987, **58**, 1544
6 Schwann, D., Mortensen, K., Springer, T., Yee-Maderia, H. and Thomas, R. *J. Chem. Phys.* 1987, **87**, 6078
7 Bates, F. S., Rosedale, J. H., Stepanek, P., Lodge, T. P., Wiltzius, P., Fredrickson, G. H. and Hjelm, R. P., Jr *Phys. Rev. Lett.* 1990, **65**, 1893
8 Stepanek, P., Lodge, T. P., Kedrowski, C. and Bates, F. S. *J. Chem. Phys.* 1991, **94**, 8289
9 Hair, D. W., Hobbile, E. K., Nakatani, A. I. and Han, C. C. *J. Chem. Phys.* 1992, **96**, 9133

10 Chu, B., Ying, Q., Linliu, K., Xie, P., Gao, T., Li, Y., Nose, T. and Okada, M. *Macromolecules* 1992, **25**, 7382
11 Broseta, D., Leibler, L. and Joanny, J. F. *Macromolecules* 1987, **20**, 1935
12 Benmouna, M., Seil, J., Meier, G., Patkowski, A. and Fischer, E. W. *Macromolecules* 1993, **26**, 668
13 Anisimov, M. A. and Kiselev, S. B. *Sov. Tech. Rev. Sec. (B) Therm. Phys.* 1992, **3** (2), 1
14 Fisher, M. E. *Phys. Rev.* 1968, **176**, 257
15 Ohbayashi, K. and Chu, B. *J. Chem. Phys.* 1978, **68**, 5066
16 Varma, K. V., Fujita, Y., Takahashi, M. and Nose, T. *J. Polym. Sci., Polym. Phys. Edn.* 1984, **22**, 1781
17 Pecora, R. 'Dynamic Light Scattering', Plenum, New York, 1985
18 Shanks, J. G. and Sengers, J. V. *Phys. Rev. (A)* 1988, **38**, 885
19 Davis, R. Y., Jr and Sciessler, R. W. *J. Am. Chem. Soc.* 1953, **75**, 2763
20 Kaddour, L. O., Anasagasti, M. S. and Strazielle, C. *Makromol. Chem.* 1987, **188**, 2223
21 Kaddour, L. O. and Strazielle, C. *Polymer* 1992, **33**, 899
22 Okada, M., Numasawa, N. and Nose, T. *Polym. Commun.* 1988, **29**, 294
23 Higashida, N., Kressler, J., Yukioka, S. and Inoue, T. *Macromolecules* 1992, **25**, 5259
24 Higashida, N., Shiomoai, K., Kressler, J. and Inoue, T. *Polym. Prepr. Japan* 1992, **41** (9), 3816
25 Broseta, D., Leibler, L., Lapp, A. and Strazielle, C. *Europhys. Lett.* 1986, **2**, 733
26 des Cloizeaux, J. and Noda, I. *Macromolecules* 1982, **15**, 1505
27 Numasawa, N., Hamada, T. and Nose, T. *J. Polym. Sci., Polym. Lett. Edn.* 1985, **23**, 1